Stable mode-locked Yb-fiber laser with a 6 MHz repetition rate tuning range

Zhao Sicong[1], Qin Peng[2], Yan Dongyu[1], Liu Bowen[1*], Wang Hongrui[1],
Song Youjian[1], Wang Sijia[2*], Hu Minglie[1]

(1. Key Laboratory of Opto-electronic Information Science and Technology of Ministry of Education, Ultrafast Laser Laboratory, School of Precision Instruments and Opto-electronics Engineering, Tianjin University, Tianjin 300072, China;
2. Qian Xuesen Laboratory of Space Technology, China Academy of Space Technology, Beijing 100094, China)

Abstract: For the precise measurement, a femtosecond mode-locked Yb-doped fiber laser with a 6 MHz repetition rate tuning range at a fundamental repetition rate of 26 MHz was reported, corresponding to 23% tuning ratio. With chirped fiber Bragg grating, the mode-locked fiber laser could run at different dispersion regimes. The influence of the net cavity dispersion on output characteristics and repetition rate tunability was studied. In a range of negative cavity dispersion, the mode-locked fiber laser could output the nearly same spectrum when the repetition rate was tuned, and the output spectrum was nearly Gaussian-type. Based on this result, a simple scheme, spatial optical path structure, and optimized cavity parameters was designed, which promised the large tunable range and stable mode-locking. The mode-locked fiber could stably output 3.23 mW ultrashort laser pulses with 347 fs dechirped pulse duration. Furthermore, the Yb-fiber laser was locked to the Rb atomic clock so that the repetition rate could be stabilized. The Allan deviation is 2×10^{-10} when the average time was 1 s.

Key words: femtosecond laser; repetition rate tuning; dispersion regime; locking system
CLC number: TN241 **Document code:** A **DOI:** 10.3788/IRLA20200205

6 MHz 重频调谐范围的稳定锁模掺镱光纤激光器

赵思聪[1], 秦 鹏[2], 闫东钰[1], 刘博文[1*], 王红蕊[1], 宋有建[1], 王思佳[2*], 胡明列[1]

(1. 天津大学 精密仪器与光电子工程学院 超快激光研究室
光电信息技术教育部重点实验室, 天津 300072;
2. 中国空间技术研究院 钱学森空间技术实验室, 北京 100094)

摘 要: 针对精密测量的实际应用需求,开发了具有 6 MHz 重复频率调谐范围的掺镱锁模光纤激光器。该光纤激光器利用啁啾光纤光栅实现色散补偿,可以实现不同色散域的锁模。实验中,系统研究了不同腔内净色散对锁模激光器输出特性和稳定性的影响,发现当具有一定负腔内净色散时,在不同的重复频率下都可以输出相同的光谱,同时输出光谱具有较好的高斯型。根据以上研究,特殊设计了稳定的简化腔结构和空间延迟线,同时优化了腔参数,保证了大范围的重复频率调谐和稳定的锁模运转。当中心重复频率为 26 MHz 时,调谐比率达到 23%。激光器稳定输出平均功率为 3.23 mW 的飞秒

收稿日期: 2020−06−03; **修订日期:** 2020−07−09
基金项目: 国家自然科学基金 (U1730115, 61805174, 61535009, 11527808); 等离子体物理重点实验室项目 (JCKYS2019212011); 强场激光物理国家重点实验室开放基金资助; 国防科技创新特区项目; 中国空间技术研究院自主创新课题; 中国航天科技集团科技创新研发项目

激光脉冲，去啁啾后脉冲宽度为 347 fs。基于此，将光纤锁模激光器重复频率锁定于铷原子钟，在 1 s 的平均时间内获得了 2×10^{-10} 的艾伦方差。

关键词：飞秒激光； 重复频率调谐； 色散域； 重复频率锁定

0 Introduction

Mode-locked fiber laser with tunable repetition rate has become a versatile tool in many metrological applications[1−4] due to advantages such as compact structure, long-term stability, and low cost. With an adjustable repetition rate, many new applications utilizing ultrafast laser pulses can be activated, such as distance measurement with interferometric method[5], optical coherence tomography[6], surface profile metrology[7], and so on.

To tune the repetition rate of mode-locked fiber lasers, many methods, such as controlling pump power, electro-optic modulation and incorporating chirped fiber Bragg grating (CFBG) to augment the cavity length are applied[8−10]. However, the tuning range of repetition rate of the aforementioned methods is limited. To solve this problem, the optical delay line is always used to change the cavity length[11−12]. Moreover, some new schemes are developed to enlarge the tuning range. Wu et. al. demonstrated a hybrid mode-locked Er-fiber oscillator whose repetition rate can be tuned from 101.3 to 103.0 MHz[13]. Yang et. al. developed a simply-integrated dual-comb spectrometer whose repetition rate can be tuned from 97.84 to 99.52 MHz achieved by automatic optical delay lines[14].

In this paper, we demonstrate a mode-locked fiber laser with a higher cavity length tuning freedom and higher stability, which offers 6 MHz f_{tr} (frequency tuning range) at 26 MHz repetition rate, corresponding to ~23% repetition rate tuning ratio. This is the largest tuning ratio as we have known. For working in mobile platforms, the free spatial optical path in the cavity, specially designed for a large tuning range, can effectively avoid the impact of vibration on laser operation, especially when repetition rate changes.

In the experiment, we analyzed the output spectra, dechirped pulse duration and immune ability to repetition rate change at different net cavity dispersion (NCD) to find the optimal NCD for stable operation and the following application. Based on this optimized cavity parameters, the fiber laser outputs 3.23 mW ultrashort laser pulses, with 347 fs dechirped pulse duration at 26.47 MHz repetition rate. Afterwards, we packaged the oscillator into a compact and stable mechanical structure for vibration isolation, meanwhile, the repetition rate is phase locked to Rb atomic clock. When the average time is 1 s, the Allan deviation is 2×10^{-10}.

1 Experimental setup

In the common mode-locked fiber lasers, the SESAM is mounted in free space as an end face of cavity for mode-locking. To tune the repetition rate, the position of SESAM is changed to extend or shorten spatial path. In this case, the vibration of SESAM in moving cannot be avoided, which induces fluctuation on the optical power density focused on the SESAM. As a result, the mode-locking is interrupted. To overcome this drawback, we demonstrate a special design of spatial optical path structure as shown in Fig. 1. The cavity is sigma type and consists of two free space arms, with a total length of 15 cm. The SESAM is equipped in one arm. In the other arm, the reflective mirror is attached to piezoelectric ceramic transducer (PZT, as short delay line) and mounted on a long delay line for changing the light path length. The laser pulse propagating path is described in the insert of Fig. 1. Due to this spatial optical path design, the SESAM is fixed and vibration is avoided when altering the cavity length.

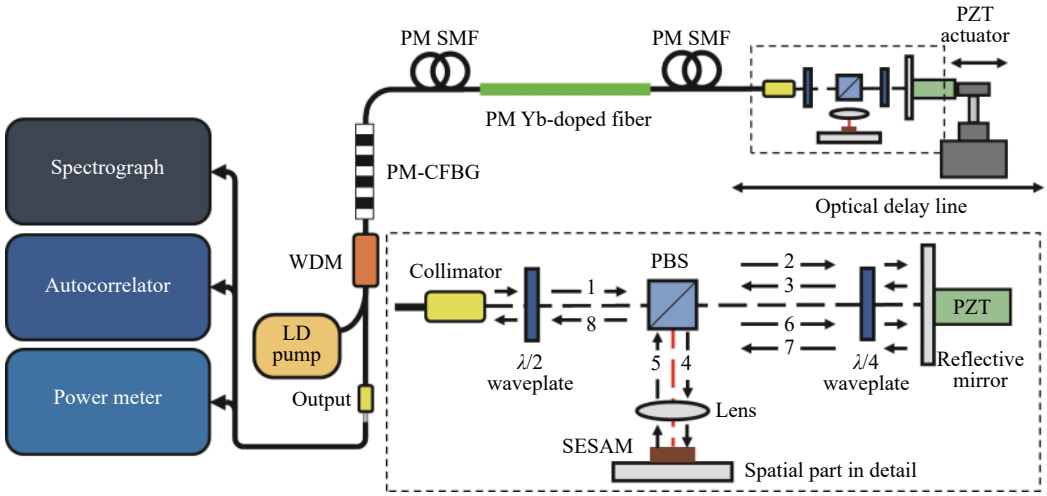

Fig.1 Schematic of mode-locked Yb-fiber laser and the details of spatial optical path. PZT, piezoelectric ceramic transducer; PBS, polarization beam splitter; SESAM, semiconductor saturable absorption mirror; PM-CFBG, polarization-maintained chirped fiber Bragg grating; PM SMF, polarization-maintained single mode fiber; WDM, wavelength division multiplexer

The SESAM (SA-1 040-26, BATOP), with 9% non-saturable loss, 26% modulation depth and 3 ps relaxation time, supports self-starting mode-locking of the fiber laser. The laser is all PM fiber structure for high environmental stabilization. The polarization-maintaining Chirped Fiber Bragg Grating (PM-CFBG) provides −0.384 2 ps^2 second-order dispersion (SOD) for compensation and ~70% output ratio. The gain fiber is Yb-doped single mode fiber (PM-YSF-HI-HP, Nufern). The length of single-mode fiber (SMF) between the Yb-doped fiber and the spatial part can be changed to adjust the NCD. The oscillator is pumped by a 976 nm diode laser.

2 Results and analysis

2.1 Analysis of laser output characteristics under different dispersion regimes

In a mode-locked fiber laser, the NCD decides mode-locking mechanisms and output parameters. In order to obtain stable operation and Gaussian-shape output spectrum for subsequent amplification, it is necessary to optimize dispersion parameters in the cavity. The multi-peak structured spectrum makes pulses accumulate complicated nonlinear phase shift in the following amplification, which can degrade the temporal quality of final dechirped pulses. However, the Gaussian-shape output spectrum can alleviate the uncompensated non-linear chirp accumulation. The negative SOD of PM-CFBG can compensate 4.36 m single mode passive fiber (PM980, β_2 = 0.022 ps^2/m). To analyze the output performance of fiber laser in different dispersion regime, different passive fiber lengths are used to adjust the NCD from -4.42×10^{-2} ps^2 to 1.70×10^{-3} ps^2, and the total fiber length is precisely measured to ensure the accuracy of NCD. In the experiment, we measured the output spectra of the pulse under maximum pump power in different dispersion regime.

In the experiment, coefficient of determination, Adjusted *R*-square, is applied to quantify the approximation degree between the spectra and its fitting Gaussian curves. When Adj. *R*-square is 1, the spectrum is Gaussian shape. Fig.2 illustrates the spectrum widths and Adj. *R*-square in different dispersion regimes. When the NCD is $< -1.29\times10^{-2}$ ps^2, the *R*-square is > 0.98, meaning that the spectral shape is nearly Gaussian-type, which benefits the following amplification and application. To analysis temporal duration of the dechirped pulse, a 1 200 line/mm grating pair is utilized to compress pulses. When the NCD is between -3.35×10^{-2} ps^2 and -2.10×10^{-2} ps^2, the dechirped pulse duration is nearly < 330 fs.

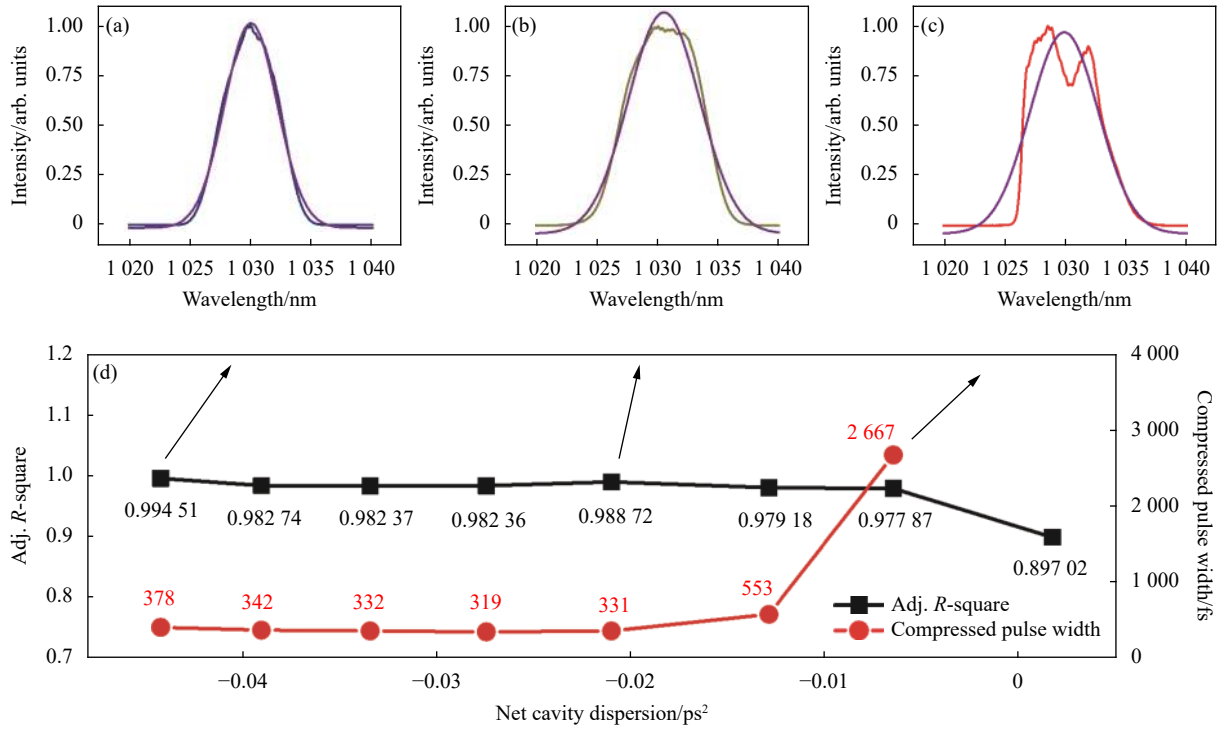

Fig.2 Dechirped pulse duration and Gaussian fitting *R*-square of output spectra when the NCD is changed from -4.42×10^{-2} ps^2 to 1.70×10^{-3} ps^2. (a) Output spectrum when NCD is -4.42×10^{-2} ps^2, FWHM=5.4 nm; (b) Output spectrum when NCD is -2.10×10^{-2} ps^2, FWHM=7.4 nm; (c) Output spectrum when NCD is -6.50×10^{-3} ps^2, FWHM=5.4 nm; (d) Dechirped pulse duration and Adj. *R*-square versus net cavity dispersion

2.2 Analysis of repetition rate tunability under different dispersion regimes

In operation, the NCD of a mode-locking fiber laser is fixed. When the repetition rate is largely tuned by altering the optical delay line with fixed pump power, the change of pulse energy in cavity cannot be ignored. As a result, output parameters fluctuate as the repetition rate tuning. In the experiment, benefiting from our spatial optical structure design, the output power changes little as the repetition rate tunes. However, we find that the change of output spectrum is far different at different NCD. The output spectra of 6 MHz f_{tr} at different NCD are shown in Fig. 3.

To analyze the consistency of output spectra, we calculated the sum of the squared errors (SSE) of a group of spectra in 6 MHz f_{tr} The SSE is the total accumulation of the squared differences between each spectrum and the average spectrum at each sampling point:

$$SSE=\sum_{i=1}^{m}\sum_{a=1}^{n}\left(I_{ai}-\bar{I}_a\right)^2 \tag{1}$$

where m is the number of the calculated spectrums and n is the number of sampling points, $\bar{I}_a$ is the average intensity at the sampling point a of the calculated spectra.

When the NCD is -2.26×10^{-2} ps^2 (Fig. 3(c)) and -3.39×10^{-2} ps^2 (Fig. 3(d)), the SSE is 1.1 and 2.3. It means that the output spectra are nearly the same within 6 MHz f_{tr}. However, the SSE becomes larger when the NCD approaches zero or becomes $<-3.39\times10^{-2}$ ps^2. It can also be demonstrated by the output spectra superposition. In Fig. 3(c) and Fig. 3(d), the curves of output spectra are overlapped well. According to the dispersion map theory[15], the pulse breathes obviously in temporal and spectral domain, when the NCD is near to zero. This means that the pulse energy perturbation in cavity can influence the breathing evolution, and pulse spectra at the output point are appreciably different. When the NCD is in negative regime, the breathing ratio is less. Meanwhile, the saturable absorber can also stabilize the pulse against perturbations. Furthermore, the optimized parameters and pulse evolution in cavity can enhance the stabilization

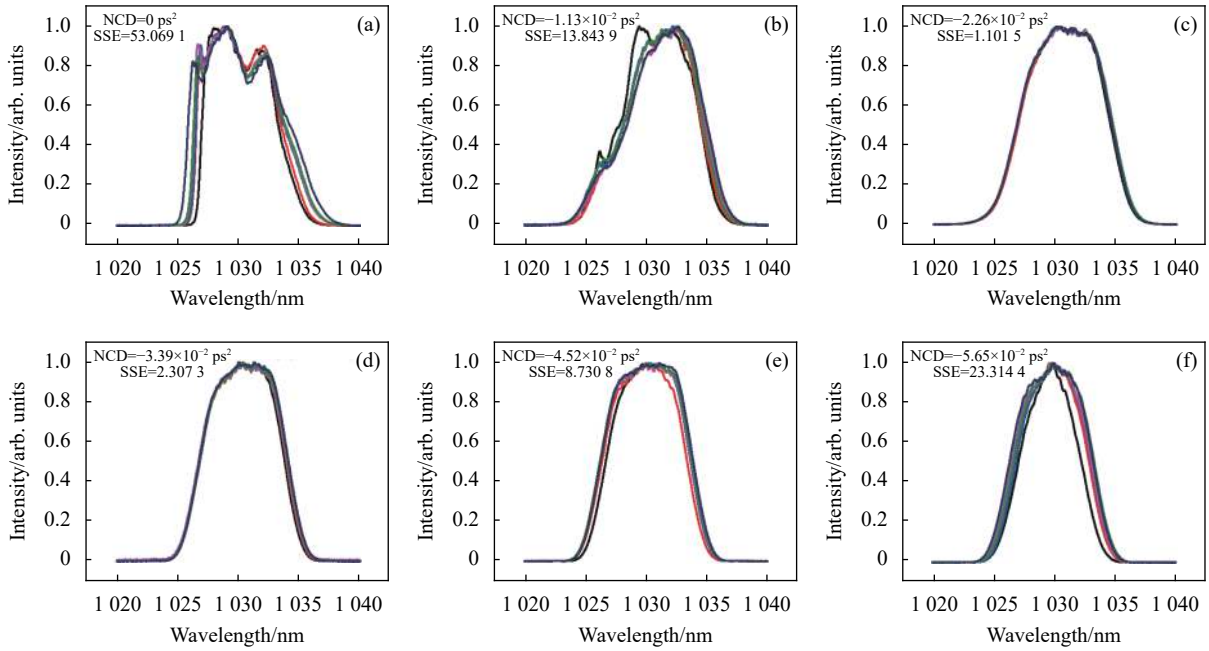

Fig.3 The output spectra and SSE values under different NCD when tuning the optical delay line. Each graph consists of 6 spectra with different repetition rate. The NCD of each graph is (a) 0 ps^2, (b) -1.13×10^{-2} ps^2, (c) -2.26×10^{-2} ps^2, (d) -3.39×10^{-2} ps^2, (e) -4.52×10^{-2} ps^2, (f) -5.65×10^{-2} ps^2, respectively

effect of SESAM. This is the reason why the SSE become larger as the NCD is $<-3.39\times10^{-2}$ ps^2.

Considering the output spectrum and dechirped pulse duration, especially the output perturbation when repetition rate tuning, the NCD can be optimized between -3.39×10^{-2} ps^2 and -2.26×10^{-2} ps^2, corresponding to a fiber length in cavity between 3.59 m and 3.85 m. The f_{tr} of both NCD are 21.83-27.72 MHz and 21.06-25.97 MHz, respectively. The tuning length of the optical delay line of both NCD are 146.10 cm and 134.66 cm, respectively. The pump power corresponding to the best output situation is 35 mW. In the experiment, the optical delay line is manually tuned, so the cavity should be refined due to manmade detuning. If the motorized linear stage is adopted in the optical delay line, this cavity detuning can be avoided.

2.3 Enhancement of repetition rate stability by locking system

Based on the experimental conclusion, we fix the NCD at -2.44×10^{-2} ps^2, which is within the ideal NCD range. Furthermore, a compact and stable mechanical structure to integrate the spatial optical path with the fiber and other devices for vibration isolation is designed, as shown in Fig. 4(b). The overall dimension of the laser is 320 mm×220 mm×65 mm. The output spectrum of the compact system is shown in Fig. 5(b). The output power is 3.23 mW @ 36 mW pump power. and repetition rate is

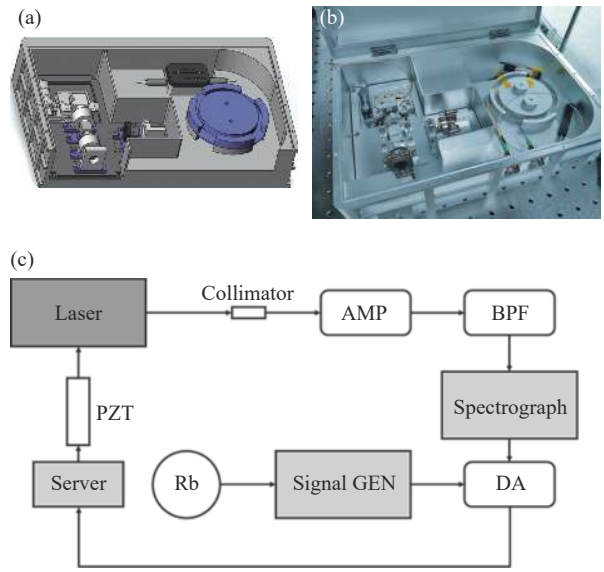

Fig.4 (a) 3-D model of the compact mechanical structure, the overall dimension is 320 mm×220 mm×65 mm. (b) Appearance of the compact laser. (c) Schematic of the repetition rate locking system

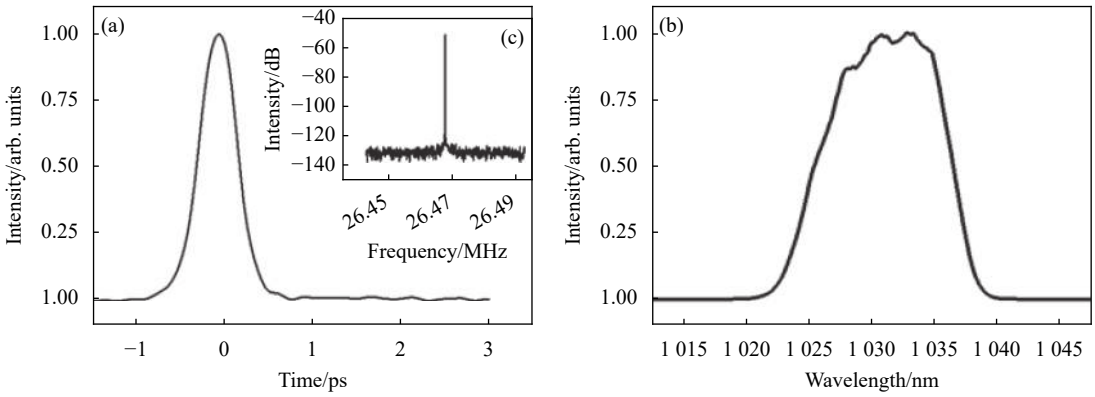

Fig.5 (a) Autocorrelation trace of the output of the compact system @36 mW pump power. (b) Output spectrum of the compact system @36 mW pump. (c) Radiofrequency spectrum of the compact system with resolution bandwidth of 30 Hz

26.47 MHz. The pulse duration directly output from the oscillator is 1.94 ps, which can be compressed to 347 fs as shown in Fig. 5(a). The chirped pulse duration is a little different from the data in Fig. 2, because the chirp of output pulses is changed slightly after the oscillator is packaged into the box. We also measured the radiofrequency spectrum, as shown in Fig. 5(c), the signal-to-noise ratio is greater than 70 dB at a resolution bandwidth of 30 Hz.

We set up a repetition rate locking system to further enhance the repetition rate stability. The feedback loop consists of a photo diode, a microwave amplifier (AMP), a band-pass filter (BPF), a signal generator (signal GEN), a Rb atomic clock (Rb), a difference frequency amplifier (DA), and a servo system (Server). The optical pulse is firstly transformed into electrical signal by the photodiode and sent to the AMP, then the high-order harmonic of the signal is selected by the BPF. We collect the 18th order harmonic of the output signal because the lower frequency signal obtains better stability when the higher harmonic maintains stable. The signal generator based on Rb atomic clock is applied as reference signal source, and the reference frequency is set to 476.403 9 MHz. The reference signal is mixed with the high-order harmonic in the DA to generate the difference frequency signal. Then, the difference signal is sent to the PI servo system to drive the PZT, so as to realize the adjustment of the repetition rate and lock it to the reference frequency.

Firstly, the oscillator works in free-running operation without locking repetition rate. The frequency meter collects the output signal for 3 000 s at a sampling interval of 10 ms. It can be observed from the Fig. 6(a) that the repetition rate continuously drifts and the maximum difference is more than 62 Hz. In the average time of 1 s, the Allan deviation is about 1×10^{-9}, as shown in Fig. 6(b), and rises with average time increasing. When the average time is 100 s, Allan deviation reaches 2×10^{-8}.

Compared with the free-running state, we then activated the repetition rate locking feedback loop to verify the effect of the feedback system. The frequency meter collects the signal for 10 000 s at the sampling interval of 10 ms. It can be observed from the Fig. 6(c) that the laser repetition rate drifts within 1.85 Hz, and the stability is improved significantly. As shown in Fig. 6(d), it is demonstrated that the Allan deviation of the laser repetition rate is about 2×10^{-10} in the average time of 1 s. With the increase of the average time, the Allan deviation decreases gradually. When the average time is 100 s, it is less than 2×10^{-11}. It should be mentioned that the curve of Allan deviation shows an upward trend around the average time of 1 000 s, which is due to the interference of low frequency vibration. However, the impact of this low frequency interference is slight, and has little unfavorable effect on the repetition rate locking.

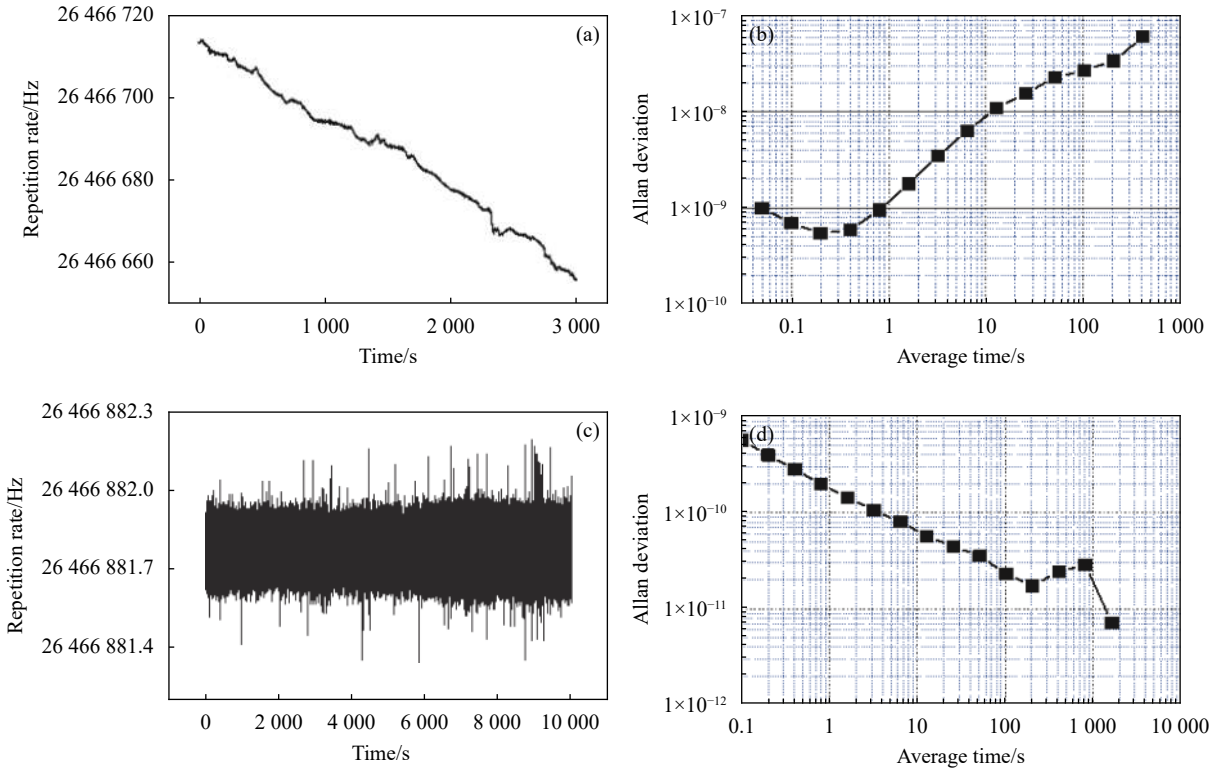

Fig.6 (a) Repetition rate of the fundamental harmonic of the output signal under free-running state. (b) Allan deviation of the repetition rate under free-running state. (c) Repetition rate of the fundamental harmonic of the output signal with feedback loop activated. (d) Allan deviation of the repetition rate with feedback loop activated

3 Conclusions

In conclusion, we demonstrate a stable mode-locked fiber laser with a 6 MHz f_{tr}, corresponding to 23% repetition rate tuning ratio. The specially designed spatial optical path is utilized to avoid impact of vibration on mode-locking, and NCD is optimized by analyzing output spectra, dechirped pulse duration and immune ability to repetition rate change. The fiber laser outputs 3.23 mW ultrashort laser pulses, with 347 fs dechirped pulse duration at 26.47 MHz repetition rate. Furthermore, the oscillator is packaged into a compact mechanical structure to isolate vibration, and the repetition rate is phase locked to Rb atomic clock at 26.47 MHz utilizing a feedback loop, the Allan deviation is restricted to 2×10^{-10} at the 1 s average time. This tunable fiber laser provides a compact and robust femtosecond laser architecture for further investigation in optical science and metrological applications.

References:

[1] Lee K, Lee J, Jang Y S, et al. Fourier-transform spectroscopy using an Er-doped fiber femtosecond laser by sweeping the pulse repetition rate [J]. ***Sci Rep***, 2015, 5: 15726.

[2] Ye Jun. Absolute measurement of a long, arbitrary distance to less than an optical fringe [J]. ***Opt Lett***, 2004, 29(10): 1153-1155.

[3] Kray S, Spöler F, Hellerer T, et al. Electronically controlled coherent linear optical sampling for optical coherence tomography [J]. ***Opt Express***, 2010, 18(10): 9976-9990.

[4] Oh J S, Kim S W. Femtosecond laser pulses for surface-profile metrology [J]. ***Opt Lett***, 2005, 30(19): 2650-2652.

[5] Wu H Z, Zhang F M, Liu T Y, et al. Absolute distance measurement using optical sampling by cavity tuning [J]. ***IEEE Photonics Technol Lett***, 2016, 28(12): 1275-1278.

[6] Villares G, Hugi A, Blaser S, et al. Dual-comb spectroscopy based on quantum-cascade-laser frequency combs [J]. ***Nat Commun***, 2014, 5: 5192.

[7] Joo W D, Kim S, Park J, et al. Femtosecond laser pulses for fast 3-D surface profilometry of microelectronic step-structures [J]. ***Opt Express***, 2013, 21(13): 15323-15334.

[8] Schibli T R, Hartl I, Yost D C, et al. Optical frequency comb with submillihertz linewidth and more than 10 W average power [J]. ***Nat Photonics***, 2008, 2(6): 355-359.

[9] Hudson D D, Holman K W, Jones R J, et al. Mode-locked fiber laser frequency-controlled with an intracavity electro-optic modulator [J]. ***Opt Lett***, 2005, 30(21): 2948-2950.

[10] Park J, Kim S, Kim B S, et al. Tuning range extension of pulse repetition rate using chirped fiber Bragg gratings [J]. ***Opt Express***, 2017, 25: 1413-1420.

[11] Hundertmark H, Kracht D, Engelbrecht M, et al. Stable sub-85 fs passively mode-locked Erbium-fiber oscillator with tunable repetition rate [J]. ***Opt Express***, 2004, 12: 3178-3183.

[12] Washburn B, Fox R, Newbury N, et al. Fiber-laser-based frequency comb with a tunable repetition rate [J]. ***Opt. Express***, 2004, 12: 4999-5004.

[13] Wu X J, Yang L J, Zhang H Y, et al. Hybrid mode-locked Er-fiber oscillator with a wide repetition rate stabilization range [J]. ***Appl Opt***, 2015, 54(7): 1681.

[14] Yang H L, Wei H Y, Chen K, et al. Simply-integrated dual-comb spectrometer via tunable repetition rates and avoiding self-referencing [J]. ***Opt Express***, 2017, 25(7): 8063-8072.

[15] Wise F W, Chong A, Renninger W H. High-energy femtosecond fiber lasers based on pulse propagation at normal dispersion [J]. ***Laser & Photon Rev***, 2008, 2(1-2): 58-73.

第一作者简介： 赵思聪，男，硕士；2013 年~2017 年就读于南开大学光电信息科学与工程 (天南大合办) 专业，获得学士学位；2017 年~2020 年在天津大学光学超快激光研究室攻读硕士学位，主要从事光纤飞秒激光器方面的研究工作。目前在华为技术有限公司工作。 Email: sczhao@tju.edu.cn

通讯作者简介： 刘博文，天津大学精密仪器与光电子工程学院，副教授，博士生导师。2009 年在天津大学获得光学工程博士学位，后留校任教。长期从事光纤飞秒激光技术与非线性光纤光学的研究，在 Optics Letters、Optics Express 等国内外高水平光学类期刊发表论文 60 余篇，其中 SCI 检索 50 篇，他引 200 次以上。获得中国百篇最具影响国际学术论文、全国优博论文提名奖、教育部技术发明一等奖等多个奖项。Email: bwliu@tju.edu.cn